Fluorescence lifetime in cardiovascular diagnostics

Laura Marcu
University of California, Davis
Department of Biomedical Engineering
Davis, California 95616

Abstract. We review fluorescence lifetime techniques including time-resolved laser-induced fluorescence spectroscopy (TR-LIFS) and fluorescence lifetime imaging microscopy (FLIM) instrumentation and associated methodologies that allow for characterization and diagnosis of atherosclerotic plaques. Emphasis is placed on the translational research potential of TR-LIFS and FLIM and on determining whether intrinsic fluorescence signals can be used to provide useful contrast for the diagnosis of high-risk atherosclerotic plaque. Our results demonstrate that these techniques allow for the discrimination of important biochemical features involved in atherosclerotic plaque instability and rupture and show their potential for future intravascular applications.
[DOI: 10.1117/1.3327279]

Keywords: fluorescence lifetime spectroscopy; fluorescence lifetime imaging microscopy (FLIM); atherosclerotic plaques; intravascular ultrasound.

Paper 09213SS received Jun. 1, 2009; accepted for publication Dec. 16, 2009; published online Mar. 1, 2010.

1 Introduction

Despite significant progress in the treatment of atherosclerotic cardiovascular disease, it results in more than 19 million deaths annually. A large number of victims of the disease die suddenly—without prior symptoms—due to plaque rupture. This critical event, to a large extent, has been associated with "vulnerable" plaque. It is well recognized[1] that existing screening and diagnostic methods are insufficient to identify the victims before the event occurs. Most techniques identify luminal diameter (stenosis), wall thickness, and plaque volume but are inefficient in identifying the rupture-prone plaque.[1–3] Consequently, new diagnostic techniques, including catheter-based techniques, to localize and characterize vulnerable plaques are of importance. It is envisioned[1] that recently developed assays (C-reactive protein), imaging techniques (CT, MRI), noninvasive electrophysiological tests, and emerging catheters in combination with genomic and proteomic techniques will guide the search for "vulnerable patients." This will potentially lead to development of new therapies and reduce the incidence of acute cardiovascular syndromes and sudden death.

Current intravascular diagnostic techniques investigated as potential tools for assessment of plaque vulnerability include nuclear magnetic resonance (NMR) spectroscopy, intravascular ultrasound (IVUS), optical coherence tomography (OCT), thermography, and spectroscopic methods.[3–22] Several optical spectroscopy techniques have been already used in atherosclerosis research, such as Raman, near-infrared (NIR), diffuse reflectance NIR, and fluorescence spectroscopy. Reviews of these techniques and studies include those by Moreno and Muller,[19] Fayad and Fuster,[20] MacNeill et al.,[3] Pasterkamp et al.,[21] and Honda and Fitzgerald.[22] These earlier studies suggest that spectroscopic techniques are highly likely to be used in the essential clinical task of identifying vulnerable plaques and that some combination of these techniques, or a combination of these techniques with other catheter-based imaging techniques such as IVUS, will be most useful.

This manuscript focuses on the potential of fluorescence lifetime spectroscopy and imaging to characterize the composition of the atherosclerotic plaques and to detect markers associated with plaque instability and rupture. In this context, we review the time-resolved laser induced fluorescence (TR-LIFS) and fluorescence lifetime imaging microscopy (FLIM) techniques developed in our laboratory and the application of these techniques to the characterization and diagnosis of human atherosclerotic plaques including coronary, aorta, and carotid arteries. In addition, we present most recent efforts on combining fluorescence lifetime spectroscopy with IVUS in a compact catheter system that facilitates simultaneous evaluation of atherosclerotic plaque composition and morphology.

2 Fluorescence Lifetime Spectroscopy and Imaging: Techniques and Methods

The fluorescence measurements have the potential to provide information about biochemical, functional, and structural changes of fluorescent biomolecular complexes in tissues and cells that occur as a result of pathological transformation.[23–34] Fluorescence spectroscopy techniques have been shown to detect elastin, collagen, lipids, and other sources of autofluorescence in normal and diseased arterial walls as well as to characterize the biochemical composition of atherosclerotic plaques both *ex vivo* and *in vivo*.[19,22,24,35–41] More recently, a few studies have reported the application of fluorescence techniques to the identification of plaque disruption,[39] detection of plaques with thin fibrous cap,[40] discrimination of lipid-rich lesions,[42] and detection of macrophage infiltration.[41,43–45] All

Address all correspondence to Laura Marcu, PhD, University of California Davis, Department of Biomedical Engineering, One Shields Avenue, Davis, CA 95616. Tel.: (530) 752-0288; Fax.: (530) 754-5739; E-mail: lmarcu@ucdavis.edu

1083-3668/2010/15(1)/011106/10/$25.00 © 2010 SPIE

of these are considered features associated with plaque vulnerability.[1]

Fluorescence measurements can be conducted as either steady state (spectrally resolved) or time resolved. The steady-state techniques for measurements of tissue autofluorescence are relatively well established.[25,31,34] However, time-resolved techniques are still evolving and are currently being actively investigated as a tool for enhanced free-label contrast in biological tissues. Such techniques are thought to improve the specificity of fluorescence measurements by resolving the fluorescence intensity decay in terms of lifetimes and thus provide additional information about the underlying fluorescence dynamics.[23,29,30] Conceptually, the fluorescence lifetime is the average time a fluorophore spends in the excited states following excitation from its ground energy level. As many of the fluorophores in biological tissues have overlapping spectra,[25,26] fluorescence lifetime properties can provide a contrast parameter. Also, the fluorescence lifetime varies with the molecular environment and is independent of fluorophore concentration and its quantum yield.[23,26,29] Overall, the use of time-resolved fluorescence for studying biological systems offers several distinct advantages, including the following:

1. Biomolecules with overlapping fluorescence emission spectra but with different fluorescence decay times can be discriminated.

2. The measurements are sensitive to various parameters of the biological microenvironment (including pH, ion concentration and binding, enzymatic activity, temperature), thus allowing these variables to be analyzed.

3. The time-resolved measurements are more robust to changes in fluorescence excitation-collection geometry; presence of endogenous absorbers (e.g., hemoglobin); photobleaching; and changes in fluorophore concentration, light scattering, and excitation intensity.

Despite these recognized inherent advantages, the potential value of fluorescence lifetime information has not been broadly implemented in clinical settings due to barriers including complexity of instrumentation, lengthy data acquisition and analysis, and high instrumentation cost. However, there is currently an increased interest in identifying solutions that enable the development of appropriate fluorescence lifetime–based instrumentation for clinical applications. In general, fluorescence lifetime information from biological system can be determined through either (1) spectroscopy systems for point measurements or (2) imaging systems known as fluorescence lifetime imaging microscopy (FLIM). In this paper, we review efforts on developing such instrumentation (point spectroscopic and imaging) and studies conducted over the past six years with this instrumentation on human atherosclerotic plaques by our research group. These studies were initiated at the Cedars-Sinai Medical Center and are currently being continued at the University of California Davis.

2.1 *Time-Resolved Fluorescence Spectroscopy–Instrumentation (Point Spectroscopy)*

The time-resolved laser-induced fluorescence spectroscopy (TR-LIFS) system developed in our lab and used in numerous studies[43,44,46,47] concerning the characterization of the biological tissues was based on a time-resolved time-domain pulse sampling and gated detection technique described in detail elsewhere.[48] It consists of a modular design including:

1. A nitrogen laser as an excitation source (337.1 nm, 700-ns pulse width, 100-mJ and 50-Hz maximum output and repetition rate, respectively).

2. A fiber-optic probe for light delivery and collection that can be implemented using various designs, including a bifurcated configuration or a single fiber coupled to a dichroic module. The fiber probe is sterilizable and includes standard fiber-optic connectors and thus requires no alignment when changing probes or light sources.

3. An f/4 dual-mode imaging spectrograph with two associated detectors.

4. A digital oscilloscope (1 GHz, sampling rate: 5 Gsamples/s), a computer workstation, and peripheral electronics.

The emitted fluorescence is captured and directed, via the collection channel of the probe, into the entrance slit of the spectrometer and detected by a multichannel plate photomultiplier tube (MCP-PMT: rise time 180 ps, spectral response 160 to 850 nm, bandwidth (BW): continuous wave (cw) to 2.0 GHz). The temporal resolution of this system is ~200 ps. The scanning monochromator allows for TR-LIFS measurements at discrete steps across the emission spectrum—an important feature when the TR-LIFS is used to characterize a new biological system (e.g., tissue type) and to determine which spectral range(s) can be used to provide useful contrast. In this initial configuration, the scanning of 200-nm (5-nm step) spectral range including the acquisition and display of fluorescence decay can be completed within approximately 30 s (~0.8 s/wavelength). The apparatus was fully contained in a modified endoscopic cart ($70\times70\times150$ cm^3) and allows for clinical research investigations. The laser triggering, the wavelength scanning, and the data acquisition, storage, and processing were controlled using a computer and custom software written in LabVIEW and MATLAB. After each measurement sequence, the laser pulse temporal profile is measured at a wavelength slightly below the excitation laser line. This profile is ulterior used as input to the deconvolution algorithm for the estimation of fluorescence lifetimes.

In the configuration described earlier, however, practical clinical application of TR-LIFS still faces challenges. These include the time-expensive data acquisition due to scanning of the monochromator. Recently, we reported[49] a novel concept that allows for near real-time acquisition of spectrally resolved fluorescence intensity transients through the combination of optical fibers and bandpass filters (Fig. 1). A single detector is used to simultaneously record multiple fluorescence intensity decay profiles (fluorescence response pulses) in response to a single pulse excitation event. Simultaneous time- and wavelength-resolved fluorescence spectroscopy (STWRFS) allows the recording of both fluorescence lifetime and spectral intensity information within hundreds of nanoseconds within multiple spectral bands. This system can be optimized for the characterization of the atherosclerotic tissue within suitable spectral bands, thus simplifying the data analysis and tissue classification algorithms. Since the objective of medical diagnosis is to identify conditions in tissue by rapidly recognizing signatures corresponding to specific states, this approach has the inherent potential for a direct

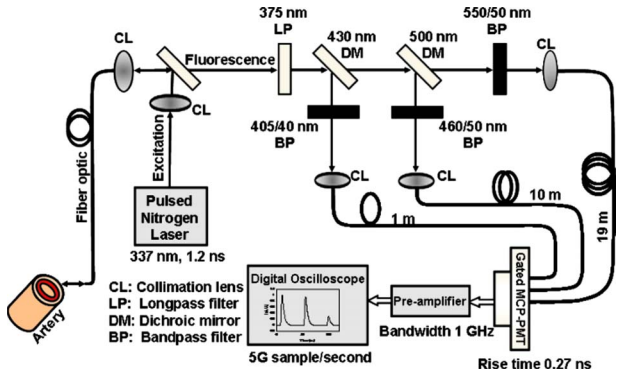

Fig. 1 Schematic of the simultaneous time- and wavelength resolved fluorescence spectroscopy (STWRFS) system. By combining multiple bandpass and dichroic filters (405/40, 460/50, and 550/50) with different lengths of optical fiber (1, 10, and 19 m) acting as optical delay, this system enables the near real-time acquisition and characterization of time-resolved fluorescence spectra using a single detector and excitation input. The recording of multiple fluorescence response pulses at selected wavelengths can be completed in hundreds of nanoseconds, which provides the capability of a real-time characterization of tissues. Configuration adapted for single-fiber excitation-collection geometry. The initial system was reported in Ref. 49.

recording of representative tissue fluorescence features. Once this apparatus is interfaced with classification models that enable online diagnosis, the STWRFS device can evolve into a clinical diagnosis tool. This research direction is currently being pursued in our laboratory and includes application of this apparatus for cardiovascular diagnostics.

2.2 *Fluorescence Lifetime Imaging Microscopy (FLIM)—Instrumentation*

In contrast to point spectroscopy systems, FLIM allows the localization and mapping of fluorophore distributions so that structural, chemical, and environmental information may be contrasted across the field of interest. The FLIM apparatus (Fig. 2) constructed in our lab was recently reported[50] and consists of a gated intensified CCD camera (ICCD), a pulsed laser, a flexible fiber-optics-based endoscope, and a filter wheel. Tissue autofluorescence is induced by 337-nm laser with 700-ps pulse width (nitrogen laser, MNL 205, LTB Lasertechnik Berlin, Germany) and collected using a graded-refractive-index (GRIN) lens (GRINTECH GmbH, Jena, Germany, NA 0.5, 0.5-mm diameter, 4-mm field of view) cemented to a fiber bundle (0.6 mm diameter, 2 m long, 10,000 fibers). For intravascular compatibility, the probe was made to be side viewing by cementing a BK7 90-deg 0.5-mm edge length polar prism on top of a GRIN objective lens. A 20× microscope objective is used to magnify fluorescence images to the ICCD. An electronically changeable filter wheel enables the selection of up to six emission wavelengths. Advanced electro-optics and fiber optics enabled the compact and robust design of this FLIM apparatus. One of the key components is the compact ICCD 4 Picos (Stanford Computer Optics, Berkeley, California) with fully integrated electronic and optical devices in a small enclosure ($24 \times 14 \times 11$ cm^3). It includes a multichannel plate (MCP) image intensifier (gate time down to 0.2 ns, repetition rate 200 kHz).

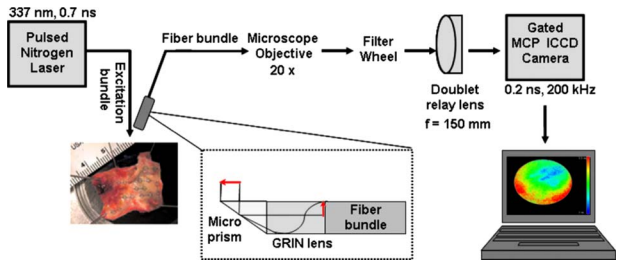

Fig. 2 Schematic of the FLIM experimental setup to transmit the 4-mm field of view at 4-mm working distance through the 10,000 coherent fiber bundle (0.5-mm outer bundle diameter) attached to the graded index (GRIN) objective lens and onto the gated camera. Adapted from Ref. 50.

2.3 *Time-Resolved Fluorescence Spectroscopy/Imaging—Data Analysis Methods*

In the context of time-domain time-resolved fluorescence measurements, the fluorescence impulse response function (FIRF) contains all the temporal information of a single fluorescence decay measurement. Mathematically, the measured fluorescence intensity decay is the convolution of the IRF with the instrument response. Thus, to estimate the FIRF of a sample, the instrument response must be deconvolved from the measured fluorescence intensity pulse.[51] Traditionally, the most commonly applied deconvolution method is the least-square iterative reconvolution (LSIR).[51,52] LSIR applies nonlinear least-square optimization methods (i.e., Gauss-Newton, Lavenberg-Marquardt) to estimate the parameters of a multiexponential IRF that would best fit its convolution with the system response to the fluorescence decay data. Since the optimization process involves iterative convolutions, LSIR is computationally expensive. Moreover, since exponential functions do not form an orthonormal basis, different multiexponential expressions can be fitted to fluorescence decay data equally well, due to the correlation of the fitting parameters in the multiexponential model. As noted earlier, fluorescence emission in tissues originates from several endogenous fluorophores and is affected by light absorption and scattering. From such a complex medium, it is not entirely adequate to analyze time-resolved fluorescence decay in terms of multiexponential components, since they cannot be always interpreted in terms of fluorophore content or number of lifetime components.[23] Thus, for tissue fluorescence lifetime data analysis, there is an advantage in avoiding any *a priori* assumption about the functional form of the IRF decay.

Consequently, we applied an alternative model-free deconvolution method for TR-LIFS data analysis, based on the Laguerre expansion of the kernel technique (LET).[53,54] This method was found to provide important advantages over the more traditional methods when used in the context of tissue characterization. LET is based on the expansion of the kernels (IRF, for linear systems) on a set of ortho-normal discrete Laguerre functions (DLFs), allowing fast converging kernel estimation from short input-output data records using least-square calculation of the expansion coefficients. Taking advantage of the asymptotic exponential decline characteristics of the DLFs, the LET was recently adapted for the deconvolution of TR-LIFS and FLIM decay data and estimation of

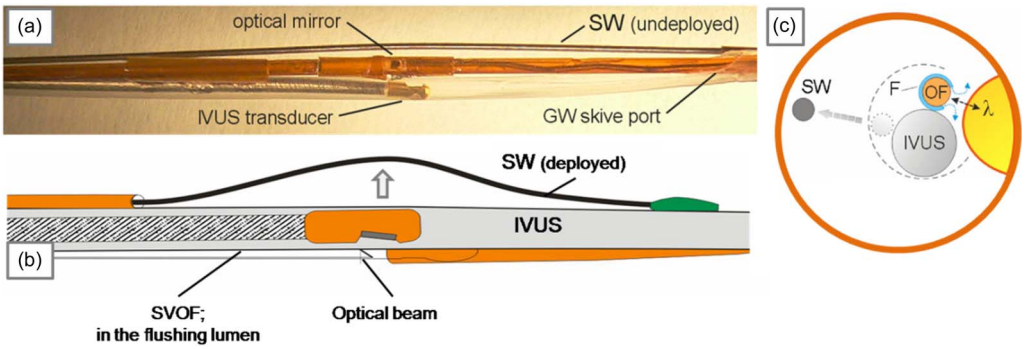

Fig. 3 (a) Picture, (b) schematic, and (c) cross section of the three components: 400-μm side-viewing optic fiber (OF); 3 Fr IVUS catheter; and 356-mm steering wire. These three components are integrated in a 5.4-Fr multimodal catheter (MMC). (b) and (c) show deployment of lateral (steering) movement with the steering wire (SW). The normally compact multimodal catheter components are separated in the photo for clearer viewing. The SW in the deployed state (b) is near the IVUS sheath and is mounted so that deployment by pushing on the wire will move the multimodal catheter close to the target. Adapted from Ref. 58.

fluorescence IRFs.[42,43,50,53,55,56] The resulting Laguerre deconvolution method has been proven to be a fast, robust, and model-free alternative for the analysis of time-resolved fluorescence data, properties highly desirable for tissue diagnostic applications. In addition, we have showed that the LECs can be used for direct characterization and diagnosis of tissue. We applied this method in the characterization of the fluorescence decay from atherosclerotic plaques.[44]

In brief, we used the orthonormal Laguerre functions $b_j^{\alpha}(n)$ to expand the FIRF and to estimate the Laguerre expansion coefficients (LEC) c_j (Refs. 44 and 57). Once the FIRFs were estimated for each emission wavelength, the steady-state spectrum (I_λ), was computed by integrating each intensity decay curve as a function of time. Further, to characterize the temporal dynamics of the fluorescence decay, two sets of parameters were used: (1) the average lifetime (τ_f) computed as the interpolated time at which the FIRF decays to 1/e of its maximum value; and (2) the normalized value of the corresponding LECs. Thus, a complete description of each sample fluorescence as a function of emission wavelength, λ_E, was given by the variation of a set of spectroscopic parameters (I_λ, τ_f, and LECs).

2.4 *Intraluminal Catheter for Combined TR-LIFS and IVUS*

As noted earlier, a combination of optical spectroscopy parameters that provideds biochemical information and imaging technique that provides structural information could provide a more complete evaluation of features involved in plaque vulnerability. As a first step in validating such an approach, we have developed[58] a novel approach that enables integration of optical (TR-LIFS) and ultrasound (IVUS) modalities to operate in a beneficial and complementary way in a single multimodal catheter (Fig. 3). IVUS is a commonly used catheter-based ultrasonic imaging technique to diagnose and guide interventional therapeutic procedures with real-time arterial cross-section images. It provides specific lesion site identification and can provide direct guidance to an intraluminal location, and subsequent relocation, of specific lesion sites of interest. IVUS, as a catheter standard for ease of use,[59] is an obvious choice for the intraluminal guidance of the optical probe for use in obtaining TR-LIFS data from sites of suspected vulnerable plaque. Overall, a practical means to implement the TR-LIFS technique involves first an intravascular means of visual guidance for the optical fiber and second a steering method to co-register the optical fiber close to a particular arterial site in a moving blood environment. In brief, the TR-LIFS data is acquired via a side-viewing optical fiber (SVOF), which is shown in Fig. 3 as OF. It consists of a 400-μm-diam fused silica fiber (multimode, NA=0.22) with a 45-deg polished metalized mirror termination for beam deflection at 90 deg to the fiber axis. The fiber optic is coupled to a dichroic mirror, which is coupled to the TR-LIFS system in our laboratory described earlier. The IVUS imaging catheter is a 3-Fr (1-mm) mechanical rotating type (SR Pro BSC, Fremont, California) catheter that operates in the 30- to 40-MHz range with its ClearViewUltra (BSC) imaging system.

3 TR-LIFS of Human Atherosclerotic Plaques

The first steps in validating the applicability of time-resolved fluorescence to characterization and detection of compositional features associated with plaque vulnerability were to determine specific fluorescence-derived parameters that can be correlated with plaque biochemical features of interest and to establish the accuracy of detecting such features. Consequently, a number of studies were conducted in human arterial atherosclerotic samples from three major arterial beds—aorta (*ex vivo*),[56,60] coronary (*ex vivo*),[43,60] and carotid (*ex vivo* and *in vivo*).[44] In the following, we present representative results from these studies.

3.1 *Material and Methods*

In all these studies, TR-LIFS measurements were obtained with serial scanning of the monochromator across a spectral range from 360 to 550 nm in increments of 10 nm. The total acquisition time across the scanned emission spectrum was ~30 s. After each measurement sequence, the laser pulse temporal profile was measured at a wavelength slightly below the excitation laser line. This profile was later used as input to the deconvolution algorithm for the estimation of fluorescence lifetimes. Laser excitation output measured at the tip of the probe was set at 2 μJ/pulse (fluence 1.8 μJ/mm^2 per pulse,

fluence rate 54 $\mu W/mm^2$ at tissue level). This output was found as being a reasonable compromise between an adequate signal-to-noise ratio and the photobleaching of the sample.

Following TR-LIFS measurements, all spectroscopically investigated plaque areas underwent conventional histopathologic evaluation. The samples were fixed (10% buffered formalin), processed routinely, and embedded in paraffin. Four sequential 4-μm-thick cross sections were cut from each segment and were stained with hematoxylin and eosin (H&E), a trichrome/elastin method, CD68 (for macrophages), and CD45 (for leukocytes), respectively. Histopathological analysis was performed by two pathologists specialized in cardiovascular diseases and blinded to the TR-LIFS data. The composition of artery wall was assessed within a region of interest (ROI) under the ink mark, defined by the fiber-optic excitation-collection geometry (~1.1-mm illuminated diameter area at tissue surface) and the light penetration depth (~250 μm for 337 nm in arterial tissue).[42] Each section was evaluated by light microscopy.

A stepwise linear discriminant analysis (SLDA) approach was adopted to generate a classification model (discriminant functions) and for sample classification. The discriminant function analysis provides an effective means for classifying spectroscopic data of unknown origin.[61] The set of features (spectroscopic parameters) selected from the statistical analysis were used for the optimization of discriminant functions. The classification accuracy was determined using a leave-one-out cross-validation approach,[61] and then values of sensitivity (SE), specificity (SP), and overall classification performance (% of samples correctly classified) were computed.

3.2 *Aorta*

The first systematic study characterizing the time-resolved fluorescence emission of normal artery and various stages of atherosclerosis was conducted in human aortic specimens (94 samples, postmortem).[60] The Laguerre deconvolution method for TR-LIFS data analysis was applied to estimate the intrinsic fluorescence decays, from which the time-integrated fluorescence emission spectrum and fluorescence lifetime were computed. This study established that the time-resolved fluorescence emission spectra of aortic samples vary with the progression of atherosclerosis. For example, average lifetime at 390 nm gradually increased from 2.4 ± 0.1 ns (normal aorta) to 3.9 ± 0.1 ns (advanced lesions), while fluorescence intensity was markedly decreased above 430 nm in intermediate and advance lesions. Characteristic changes in parameters derived from the time-resolved spectra were related to the type of lesion assigned to the sample based on histological examination. Spectral and temporal features of the emission were interpreted for normal aortic wall and lesions ranging from early type I to advanced type V in terms of intimal content in fluorescent compounds and intimal thickness. Trends in the average lifetime at selected wavelengths were identified, which could serve as diagnostic markers for *in situ* optical analysis of the aortic wall. Also, it was determined[60] that a set of five predictors variables (fluorescence time-decay parameters at 390 nm and 460 nm and fluorescence intensity values at 490 nm) allows for discrimination of the lipid-rich lesions (rupture-prone) from collagenous/fibrous lesions (stable) with a sensitivity and specificity higher than 95%.

3.3 *Coronary Artery*

In a following study,[43,60] time-resolved fluorescence emission of normal and atherosclerotic human coronary arteries (58 coronary segments, postmortem) were analyzed using also the Laguerre deconvolution method. Similar to the study in aorta, these results showed that analysis of the time-resolved fluorescence spectra can be used to enhance the discrimination between different grades of atherosclerotic lesions as defined by the American Heart Association (AHA). Also, it demonstrated that the lipid-rich lesions (e.g., average lifetime at 390 nm: 2.6 ± 0.1 ns) can be differentiated from the other lesion types—in particular, fibrous lesions (3.2 ± 0.15 ns) and normal arterial wall (2.1 ± 0.1 ns). It was determined that spectroscopic features derived for lipid components are reflected in the emission of lipid-rich lesions, whereas characteristics of type I collagen are identified in the emission of fibrous lesions. In addition, the results suggested that a few spectroscopic parameters that combine spectral features at longer wavelengths and time-resolved characteristics from the peak emission region are the best selections for coronary artery lesion discrimination. For example, parameters derived from time-resolved spectra, such as the lifetime and the fast-time decay constants determined using a biexponential approximation of the intensity decay, are most likely to differentiate between lipid-rich (more unstable) and fibrous lesions (more stable) and be used for diagnosis. These findings further validated the potential of TR-LIFS for discriminating lipid-rich plaques from fibrotic lesions.

3.4 *Carotid Artery*

More recently,[44] we conducted a TR-LIFS study in fresh excised carotid plaques from 65 endarterectomy patients (831 distinct areas). This study was designed (1) to demonstrate whether TR-LIFS signatures can distinguish fibrotic caps rich in macrophages and inflammatory cells and plaques with a necrotic/lipid core under a thin cap (rupture-prone) from plaques with caps rich in collagen (stable); and (2) to determine the TR-LIFS derived spectroscopic parameters that can be correlated to features of plaque vulnerability. Results of this study (Fig. 4) indicated that spectral features derived from the normalized time-integrated fluorescence emission spectra provide means for discriminating early lesions or intima thickening (IT) from more advanced stable lesions such as fibrotic (FP) and fibrocalcified (FC) and unstable lesions such as inflamed (INF) and necrotic (NEC) plaques. Also, the study indicated that time-resolved properties of the autofluorescence emission enable detection of superficial necrotic core, one additional feature of plaque vulnerability.

This study also demonstrated the important role that the LECs play in atherosclerotic plaques discrimination. While in previous studies, the Laguerre deconvolution method was primarily used to estimate the intrinsic fluorescence decay emission, in this study, in addition the resulting LECs were adopted for the first time as additional parameters for quantifying the time-resolved fluorescence emission (Fig. 4). Notably, one of these expansion coefficients (LEC-2) enabled discrimination of both inflamed and necrotic lesions from the stable plaques. Moreover, a combination of spectral and time-resolved fluorescence parameters, including LECs, were used as features in a linear discriminant analysis (LDA)–based

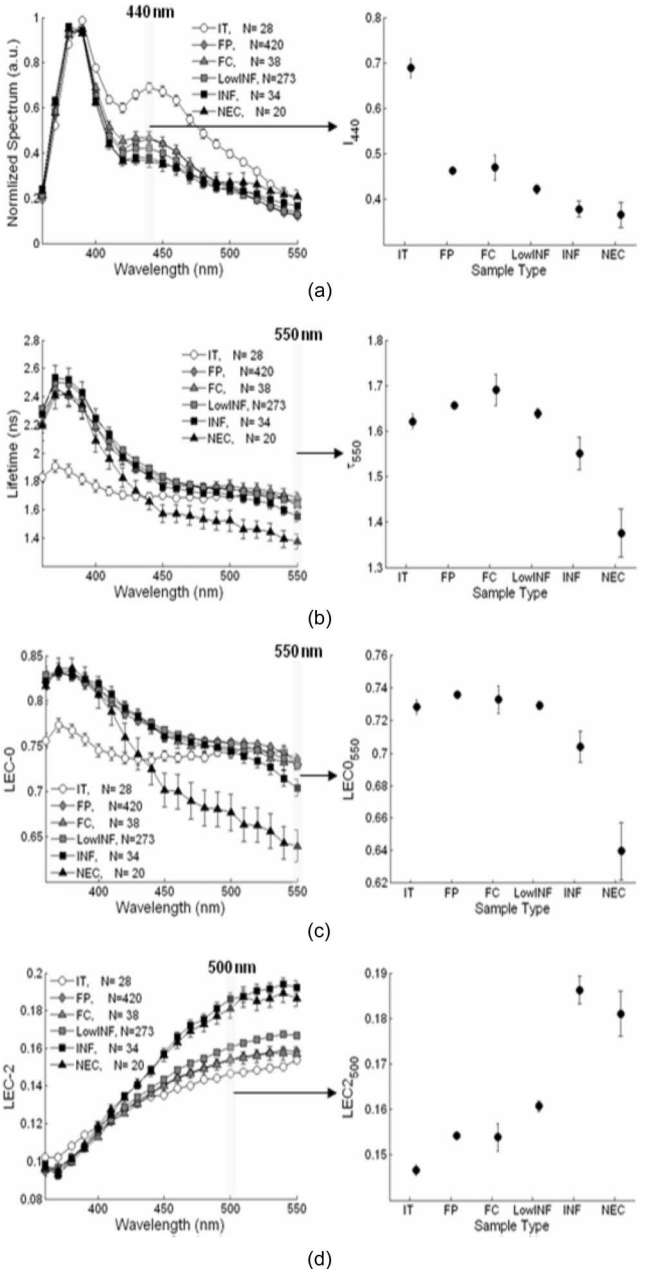

Fig. 4 Left panels: Spectroscopic parameters as a function of emission wavelength derived from the time-resolved spectra measured in *ex vivo* samples. Right panels: Statistical group comparisons (mean ± S.E.) for specific wavelengths. Spectroscopic parameters: normalized intensity (a), average lifetime (b), LEC-0 (c), and LEC-2 (d). Adapted from Ref. 44.

classifier, which was able to discern inflamed and necrotic lesions from early and advanced fibrotic lesions with high sensitivity (>80%) and specificity (>90%). Results of the classification aiming to discriminate IT, FP/FC, and INF/NEC lesions are shown in Table 1. The overall cross-validation classification performance was 74.3%. IT was discriminated with sensitivity (SE) and specificity (SP) larger than 80%. However, there was an appreciable overlap between IT and FP/FC. Also, the INF and NEC lesions were detected with high SE (larger than 80%) and high SP (larger than 90%).

Table 1 Classification accuracy (sensitivity and specificity): discrimination of IT, FP/FC, and INF/NEC (from Ref. 44).

	Fluorescence spectroscopy				
	IT	FP/FC	INF/NEC	Sensitivity (%)	Specificity (%)
IT (N=28)	25	3	0	89.3	80.7
FP/FC (N=458)	99	332	27	72.5	84.2
INF/NEC (N=54)	0	10	44	**81.5**	**94.4**

These results provide strong indication that the LECs offer a new domain for representing the time-resolved information of tissue fluorescence emission in a very compact, accurate, complete, and computationally efficient way. This study also clearly demonstrated that the LECs derived from the TR-LIFS data analysis can characterize arterial tissue composition and, most important, detect features of vulnerable plaques, such as superficial necrosis and inflammation.

This study in carotid artery demonstrated also that a linear correlation between plaque biochemical content and spectroscopic parameters can be determined. Plaque elastin content, ranging from near 0% (in the advanced FP, FC, INF, and NEC) to 50% (in IT) showed a positive correlation with the intensity values at 440-nm emission. Necrotic area, ranging from 0% (in stable plaques) to 70% (in NEC), presented a negative correlation with the LEC-0 at 550-nm emission. A similar correlation was determined for the average lifetime values. The inflammatory cell (lymphocyte/macrophage) content, ranging from 0% (in stable plaques) to 60% (in INF and NEC), showed a positive correlation with the LEC-2 at 550 nm. In contrast, LEC-2 at 550 nm was negatively correlated to the collagen/SMC content.

4 FLIM of Human Atherosclerotic Plaques

Most recently, we have investigated the ability of a fiber bundle FLIM apparatus to map the composition of human atherosclerotic plaques.[62] Using the FLIM experimental apparatus and the imaging bundle probe[50] briefly described earlier, we have conducted experiments on 10 human aorta samples obtained at autopsy. This system allows for mapping in one measurement the tissue composition within a 4-mm-diam surface with ~35-mm spatial and ~200-ps temporal resolution. Two bandpass filters were used throughout this study (central wavelength/bandwidth): 377/50 and 460/60. The FLIM images were correlated with the sample histopathologic analysis (standard H&E and elastin-trichrome stains) conducted by a pathologist. The percentage (0 to 100) of fibrosis, elastin, calcification, necrosis, cholesterol, macrophages, and lymphocytes within the 4-mm-diam by ~250-μm-depth region of interest defined by the excitation-collection geometry of the FLIM catheter and the 337-nm light penetration depth in arterial samples. Figure 5 depicts representative FLIM images for normal and atherosclerotic arteries and their corresponding fluorescence lifetime histograms. Although preliminary (a

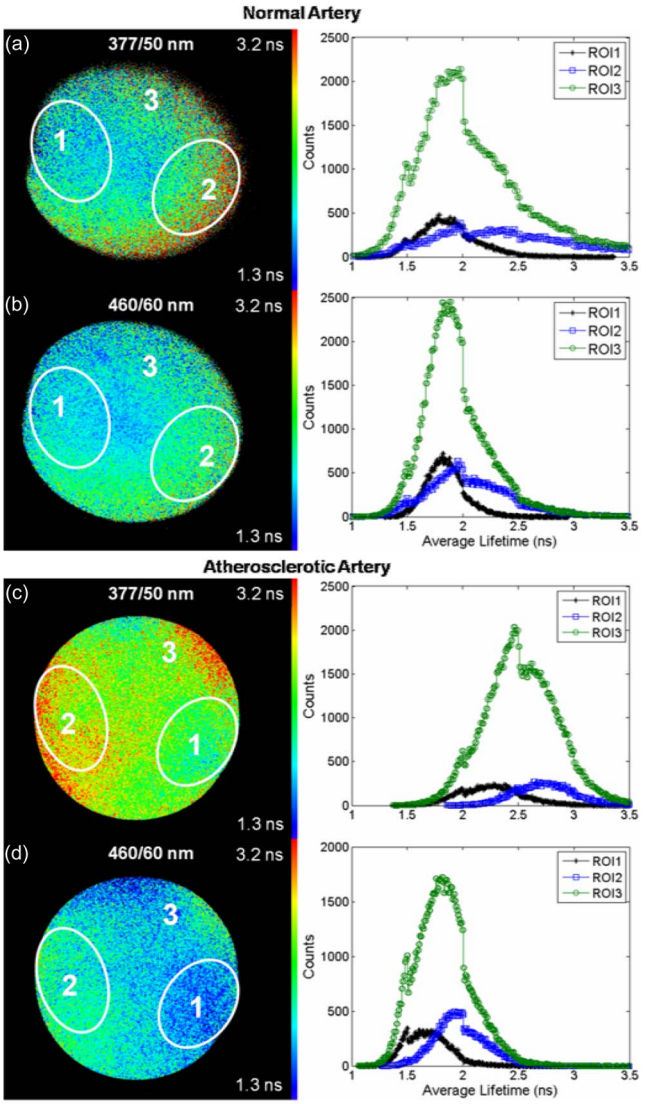

Fig. 5 FLIM images of normal artery at (a) 377/50 nm (center wavelength/bandwidth) and at (b) 460/60 nm. Note the uniformly ~2-ns average lifetimes, which is typical of elastin fluorescence. Images of atherosclerotic artery at (c) 377/50 nm and at (d) 460/60 nm. Note the longer lifetimes in (c) typical of collagen fluorescence and the shorter lifetimes in (d) typical of lipid fluorescence, indicating that this plaque has both collagen-rich (ROI 2) and lipid-rich (ROI 1) components. Histograms correspond to the images to their left.

more comprehensive study is under way and will be reported elsewhere), these early results are in agreement with those obtained using TR-LIFS. We noted the relatively uniform lifetime map (~1.8 ns) for normal artery in both spectral bands [Figs. 5(a) and 5(b)]—trends corresponding to the broad elastin fluorescence known to dominate the fluorescence of the normal artery. The fluorescence emission of the fibrotic plaque [Fig. 5(c)] was characterized by a longer lasting emission (~2.5 ns) within the blue-shifted spectral band—a feature corresponding to collagen fluorescence emission. The lifetime varied with the emission wavelength and was found to be short lasting (~1.8 ns) at the red-shifted band—a trend that was also observed in the TR-LIFS studies of human aorta.[56,60]

5 Multimodal TR-LIFS and IVUS of Human Atherosclerotic Plaques

Using the prototype multimodal catheter system described earlier (Fig. 3), we conducted experiments *in vitro*[58] and most recently *in vivo* (comprehensive results to be reported elsewhere) that demonstrate that this catheter can be used to locate a fluorophore in the vessel wall with a guiding precision of 0.53 ± 0.16 mm, steer the SVOF in place, perform blood flushing under flow conditions, and acquire robust TR-LIFS data upon UV light tissue excitation. The performance of the multimode catheter was tested in arterial phantoms made of polymethyl-methacrylate (PMMA) with wall-mounted fluorophore targets, *ex vivo* pig arteries, and *in vivo* in a femoral artery of swine. Figure 6 presents representative results from these studies. During TR-LIFS measurements, saline was flushed through the flushing tube surrounding the SVOF, as depicted in Fig. 3, at a rate of 0.07 ml/s. We noted that the TR-LIFS spectral intensity was modulated by the peak (at 415 nm) of the blood absorbance, but the time-resolved data (average lifetime values) were not affected by the blood pressure. As anticipated, this demonstrated again that fluorescence lifetime measurements are more robust than intensity measurements in the presence of endogenous absorbers such as blood. Note also that during *in vivo* experiments, the effect of blood absorbance was observed only when the catheter was not fully in contact with the arterial wall. In addition, we determined that the catheter steering capability used for the co-registration of the IVUS image plane and the SVOF beam permitted a guiding precision to an arterial wall site location of 0.53 ± 0.16 mm.

6 Conclusion

The TR-LIFS and FLIM studies conducted in all three human arterial vessel (aorta, coronary, and carotid) taken together provide ample evidence to infer that time-resolved fluorescence–based techniques can potentially become an important tool for detecting features related to plaque vulnerability during intravascular catheterization. All studies have confirmed that elastin is the major source of endogenous fluorescence in all normal arteries and early lesions, while collagen is the main source of fluorescence in more advanced lesions. Since these two endogenous fluorophores have very distinct spectral and time-resolved characteristics, discrimination between normal arterial wall and early lesions from more advanced lesions is possible using fluorescence information. These studies also indicate that lipid-rich lesions, including those with thin cap fibroatheromas and large lipid pool, and inflamed lesions with superficial foam cells can be discriminated from more stable collagen-rich lesions; however, this is based primarily on time-resolved fluorescence characteristics. In addition, these studies have demonstrated that a small subset of spectral and time-resolved parameters (less than 10 parameters) retrieved from a limited number of emission wavelengths (~4 wavelengths) can provide a means for delineating early from advanced lesions, and more important, the presence of lipid-rich lesions as well as of the inflamed fibrotic cap. This finding is particularly important, as it allows for the design of TR-LIFS and FLIM systems that collect fluorescence decay at a limited number of wavelength bands. Such systems are currently under development. For example,

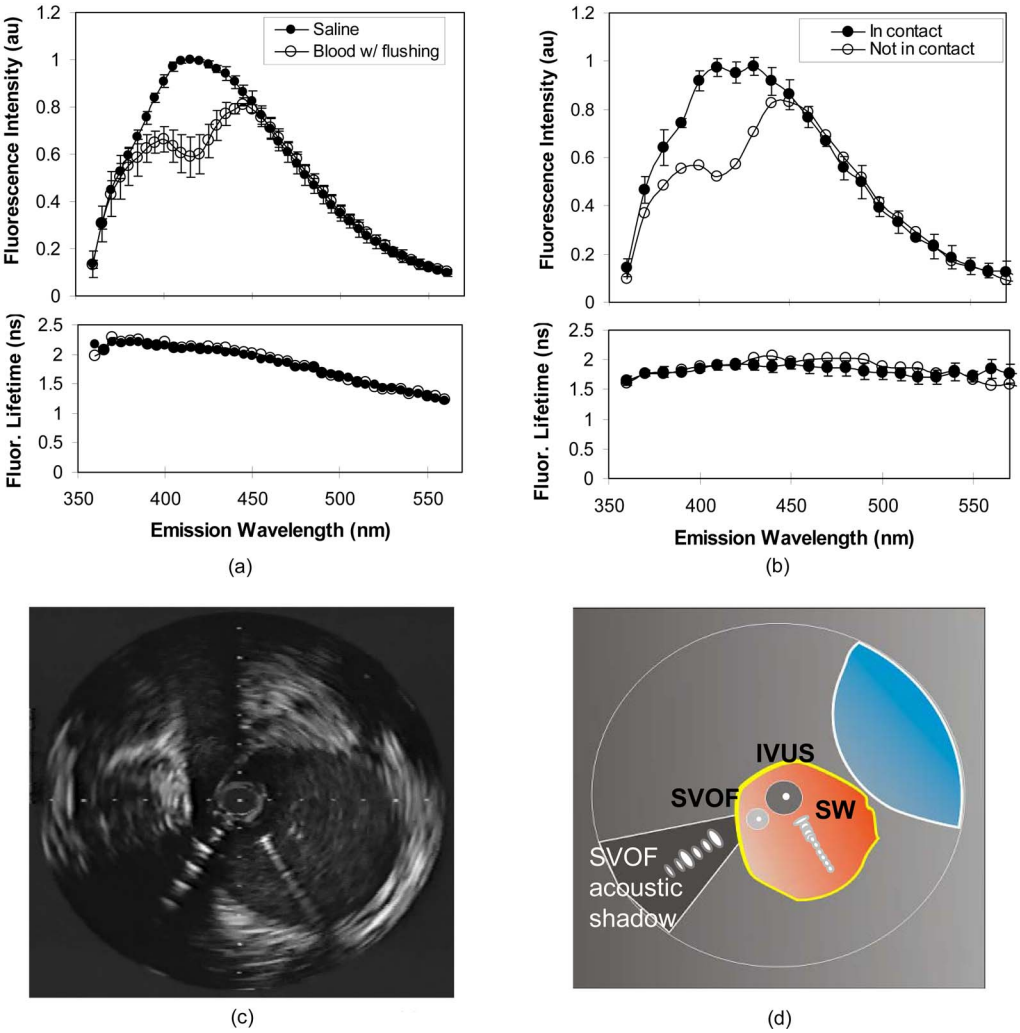

Fig. 6 TR-LIFS and IVUS using the multimodal catheter (a) *ex vivo* and (b) *in vivo*. (a) Top panel: Comparison fluorescence emission spectra from an *ex vivo* pig femoral artery for moving whole blood ($N=7$) conditions versus normalized spectral emission in saline ($N=5$). Bottom panel: The corresponding fluorescence average lifetimes along the emission spectrum. (b) Top panel: Comparison fluorescence intensity spectrum from *in vivo* pig femoral artery when the catheter is fully deployed and in contact with the arterial wall ($N=4$) versus fluorescence intensity spectrum when the catheter is not fully deployed and not in contact with the arterial wall. Bottom panel: The corresponding fluorescence lifetimes along the emission spectrum. (c) IVUS image and (d) illustration demonstrating the application of the multimodal catheter *in vivo* in pig femoral artery. The depicted condition corresponds to catheter in contact with the arterial wall. Adapted from Ref. 58.

a prototype depicting an original design for simultaneous time- and wavelength-resolved fluorescence spectroscopy was recently reported by our research group[49] (Fig. 1). This approach, which permits rapid data acquisition (hundreds of microseconds for multiple spectral bands), combined with Laguerre expansion of the kernel technique, which permits a fast deconvolution of the fluorescence decay data, can provide a means for overall data acquisition-analysis of less than 1 s—a critical feature for clinical applications.

A main limitation of fluorescence-based techniques in the evaluation of the arterial plaques is the relatively shallow UV light penetration of excitation light ($\sim 250\ \mu$m). Although UV excitation of the fluorophores in the arterial wall makes TR-LIFS and FLIM suitable methods for detection of markers of plaque vulnerability in thin fibrotic caps, it also limits the ability of this technique to assess plaque morphology associated with other markers of plaque vulnerability, such as the size of the lipid pool or expansive (positive) remodeling, or to distinguish other important features involved in plaque pathology, including pathologic intimal thickening[63] versus fibrous thick-cap atheroma. Such limitations, however, can be further addressed though complementary imaging techniques. As suggested earlier[1] for other spectroscopic methods currently being evaluated for clinical diagnosis of vulnerable plaques (e.g., NIR and Raman spectroscopy), an optimum approach to vulnerable plaque detection would need to incorporate structural definition of a high-resolution modality (e.g., OCT, intravascular MRI, or high-frequency IVUS) with biochemical processes detected by optical spectroscopy (e.g., TR-LIFS). Our current efforts on developing catheters that integrate TR-LIFS and IVUS are specifically designed to address this need. Current results demonstrate that such integration is feasible. Moreover, IVUS can be used to guide the spectroscopic investigations. Further translation of the bi-

modal TR-LIFS and IVUS technique to intraluminal investigation of arterial wall in clinical settings would require, however, validation of this approach in pre-clinical studies of animal models of atherosclerosis in blood flow; extensive correlation of the fluorescence/ultrasonic data with the biochemical/morphological features derived via standard histopathologic and immunohistochemistry methods; and development of classification models that allow for integration of features derived from the two modalities for a better prediction of markers of plaque vulnerability. Our current research efforts target such endeavors.

In addition, due to its ability to detect the compositional makeup of the arterial wall, another potential application of TR-LIFS is the clinical management of stenting procedures. Knowledge of arterial wall composition at the time of percutaneous coronary interventions may allow the physician to "personalize" the selection of the type of stent (e.g., uncoated or drug-eluting), thus more effectively reducing the risk of restenosis and target-vessel revascularization. Also, the sensitivity of TR-LIFS measurement to the arterial wall content in structural proteins suggests the potential application of this technique in assessing the effect of experimental drugs in plaque regression and stabilization. Thus, TR-LIFS may also play an important role in drug-discovery studies *in vivo* in animal models.

Acknowledgments

We thank all contributors to the studies presented in this manuscript including graduate students, postdoctoral fellows, and collaborators: Drs. Yang Sun, Daniel S. Elson, Yinghua Sun, Hongtao Xie, Douglas N. Stephens, Jenifer Phipps, Thanassis Papaioannou, Javier A. Jo, Qiyin Fang, Jesung Park, Nisa Hatami, and Matthew Yee. Clinical collaborators: Drs. Michael C. Fishbein, Julie A. Freischlag, J. Dennis Baker, J.-H. Qiao, and Ramez Saroufeem. This work was supported in part by the National Institute of Health Grant R01 HL 67377.

References

1. M. Naghavi, P. Libby, E. Falk, S. W. Casscells, S. Litovsky, J. Rumberger, J. J. Badimon, C. Stefanadis, P. Moreno, G. Pasterkamp, Z. Fayad, P. H. Stone, S. Waxman, P. Raggi, M. Madjid, A. Zarrabi, A. Burke, C. Yuan, P. J. Fitzgerald, D. S. Siscovick, C. L. de Korte, M. Aikawa, K. E. Juhani Airaksinen, G. Assmann, C. R. Becker, J. H. Chesebro, A. Farb, Z. S. Galis, C. Jackson, I. K. Jang, W. Koenig, R. A. Lodder, K. March, J. Demirovic, M. Navab, S. G. Priori, M. D. Rekhter, R. Bahr, S. M. Grundy, R. Mehran, A. Colombo, E. Boerwinkle, C. Ballantyne, W. Insull Jr., R. S. Schwartz, R. Vogel, P. W. Serruys, G. K. Hansson, D. P. Faxon, S. Kaul, H. Drexler, P. Greenland, J. E. Muller, R. Virmani, P. M. Ridker, D. P. Zipes, P. K. Shah, and J. T. Willerson, "From vulnerable plaque to vulnerable patient: a call for new definitions and risk assessment strategies: part I," *Circulation* **108**(14), 1664–1672 (2003).
2. P. Libby and M. Aikawa, "Stabilization of atherosclerotic plaques: new mechanisms and clinical targets," *Nat. Med.* **8**(11), 1257–1262 (2002).
3. B. D. MacNeill, H. C. Lowe, M. Takano, V. Fuster, and I. K. Jang, "Intravascular modalities for detection of vulnerable plaque: current status," *Arterioscler., Thromb., Vasc. Biol.* **23**(8), 1333–1342 (2003).
4. G. J. Tearney, H. Yabushita, S. L. Houser, H. T. Aretz, I. K. Jang, K. H. Schlendorf, C. R. Kauffman, M. Shishkov, E. F. Halpern, and B. E. Bouma, "Quantification of macrophage content in atherosclerotic plaques by optical coherence tomography," *Circulation* **107**(1), 113–119 (2003).
5. I. K. Jang, G. Tearney, and B. Bouma, "Visualization of tissue prolapse between coronary stent struts by optical coherence tomography—comparison with intravascular ultrasound," *Circulation* **104**(22), 2754 (2001).
6. T. S. Hatsukami, R. Ross, N. L. Polissar, and C. Yuan, "Visualization of fibrous cap thickness and rupture in human atherosclerotic carotid plaque *in vivo* with high-resolution magnetic resonance imaging," *Circulation* **102**(9), 959–964 (2000).
7. G. G. Zimmermann, P. Erhart, J. Schneider, G. K. von Schulthess, M. Schmidt, and J. F. Debatin, "Intravascular MR imaging of atherosclerotic plaque: *ex vivo* analysis of human femoral arteries with histologic correlation," *Radiology* **204**(3), 769–774 (1997).
8. C. L. de Korte, S. G. Carlier, F. Mastik, M. M. Doyley, A. F. W. van der Steen, P. W. Serruys, and N. Bom, "Morphological and mechanical information of coronary arteries obtained with intravascular elastography—feasibility study *in vivo*," *Eur. Heart J.* **23**(5), 405–413 (2002).
9. F. S. Foster, C. J. Pavlin, K. A. Harasiewicz, D. A. Christopher, and D. H. Turnbull, "Advances in ultrasound biomicroscopy," *Ultrasound Med. Biol.* **26**(1), 1–27 (2000).
10. I. K. Jang, G. J. Tearney, D. H. Kang, Y. C. Moon, S. J. Park, S. W. Park, K. B. Seung, S. L. Houser, M. Shishkov, E. Pomerantsev, H. T. Aretz, and B. E. Bouma, "Comparison of optical coherence tomography and intravascular ultrasound for detection of coronary plaques with large lipid-core in living patients," *Circulation* **102**(18), 509 (2000).
11. S. Maruvada, K. K. Shung, and S. H. Wang, "High-frequency backscatter and attenuation measurements of porcine erythrocyte suspensions between 30–90 MHz," *Ultrasound Med. Biol.* **28**(8), 1081–1088 (2002).
12. Y. Saijo and A. F. W. Steen, *Vascular Ultrasound*, Springer, Tokyo (2003).
13. P. G. Yock and P. J. Fitzgerald, "Intravascular ultrasound: state of the art and future directions," *Am. J. Cardiol.* **81**(7A), 27e–32e (1998).
14. B. E. Bouma, G. J. Tearney, H. Yabushita, M. Shishkov, C. R. Kauffman, D. D. Gauthier, B. D. MacNeill, S. L. Houser, H. T. Aretz, E. F. Halpern, and I. K. Jang, "Evaluation of intracoronary stenting by intravascular optical coherence tomography," *Heart* **89**(3), 317–320 (2003).
15. J. G. Fujimoto, S. A. Boppart, G. J. Tearney, B. E. Bouma, C. Pitris, and M. E. Brezinski, "High resolution *in vivo* intra-arterial imaging with optical coherence tomography," *Heart* **82**(2), 128–133 (1999).
16. S. Verheye, G. R. Y. De Meyer, G. Van Langenhove, M. W. M. Knaapen, and M. M. Kockx, "*In vivo* temperature heterogeneity of atherosclerotic plaques is determined by plaque composition," *Circulation* **105**(13), 1596–1601 (2002).
17. W. Casscells, B. Hathorn, M. David, T. Krabach, W. K. Vaughn, H. A. McAllister, G. Bearman, and J. T. Willerson, "Thermal detection of cellular infiltrates in living atherosclerotic plaques: possible implications for plaque rupture and thrombosis," *Lancet* **347**(9013), 1447–1449 (1996).
18. C. Stefanadis, K. Toutouzas, M. Vavuranakis, E. Tsiamis, D. Tousoulis, D. B. Panagiotakos, S. Vaina, C. Pitsavos, and R. Toutouzas, "Statin treatment is associated with reduced thermal heterogeneity in human atherosclerotic plaques," *Eur. Heart J.* **23**(21), 1664–1669 (2002).
19. P. R. Moreno and J. E. Muller, "Identification of high-risk atherosclerotic plaques: a survey of spectroscopic methods," *Curr. Opin. Cardiol.* **17**(6), 638–647 (2002).
20. Z. A. Fayad and V. Fuster, "Clinical imaging of the high-risk or vulnerable atherosclerotic plaque," *Circ. Res.* **89**(4), 305–316 (2001).
21. G. Pasterkamp, E. Falk, H. Woutman, and C. Borst, "Techniques characterizing the coronary atherosclerotic plaque: influence on clinical decision making," *J. Am. Coll. Cardiol.* **36**(1), 13–21 (2000).
22. Y. Honda and P. J. Fitzgerald, "Frontiers in intravascular Imaging technologies," *Circulation* **117**(15), 2024–2037 (2008).
23. J. R. Lakowicz, *Principles of Fluorescence Spectroscopy*, 2nd ed., Kluwer Academic/Plenum, New York (1999).
24. R. Richards-Kortum and E. Sevick-Muraca, "Quantitative optical spectroscopy for tissue diagnosis," *Annu. Rev. Phys. Chem.* **47**, 555–606 (1996).
25. G. A. Wagnieres, W. M. Star, and B. C. Wilson, "*In vivo* fluorescence spectroscopy and imaging for oncological applications," *Photochem. Photobiol.* **68**(5), 603–632 (1998).
26. M.-A. Mycek and B. W. Pogue, Eds., *Handbook of Biomedical Fluorescence*, Marcel Dekker, New York (2003).

27. S. Andersson Engels, C. Klinteberg, K. Svanberg, and S. Svanberg, "*In vivo* fluorescence imaging for tissue diagnostics," *Phys. Med. Biol.* **42**(5), 815–824 (1997).
28. I. J. Bigio and J. R. Mourant, "Ultraviolet and visible spectroscopies for tissue diagnostics: fluorescence spectroscopy and elastic-scattering spectroscopy," *Phys. Med. Biol.* **42**(5), 803–814 (1997).
29. R. Cubeddu, D. Comelli, C. D'Andrea, P. Taroni, and G. Valentini, "Time-resolved fluorescence imaging in biology and medicine," *J. Phys. D* **35**(9), R61–R76 (2002).
30. B. B. Das, F. Liu, and R. R. Alfano, "Time-resolved fluorescence and photon migration studies in biomedical and model random media," *Rep. Prog. Phys.* **60**(2), 227–292 (1997).
31. R. A. Drezek, R. Richards-Kortum, M. A. Brewer, M. S. Feld, C. Pitris, A. Ferenczy, M. L. Faupel, and M. Follen, "Optical imaging of the cervix," *Cancer* **98**(9), 2015–2027 (2003).
32. T. Glanzmann, J. P. Ballini, H. van den Bergh, and G. Wagnieres, "Time-resolved spectrofluorometer for clinical tissue characterization during endoscopy," *Rev. Sci. Instrum.* **70**(10), 4067–4077 (1999).
33. M. A. Mycek, K. T. Schomacker, and N. S. Nishioka, "Colonic polyp differentiation using time-resolved autofluorescence spectroscopy," *Gastrointest. Endosc.* **48**(4), 390–394 (1998).
34. N. Ramanujam, "Fluorescence spectroscopy of neoplastic and non-neoplastic tissues," *Neoplasia* **2**(1–2), 89–117 (2000).
35. T. G. Papazoglou, W. Q. Liu, A. Katsamouris, and C. Fotakis, "Laser-induced fluorescence detection of cardiovascular atherosclerotic deposits via their natural emission and hypocrellin (Ha) probing," *J. Photochem. Photobiol., B* **22**(2), 139–144 (1994).
36. A. J. Morguet, B. Korber, B. Abel, H. Hippler, V. Wiegand, and H. Kreuzer, "Autofluorescence spectroscopy using Xecl excimer-laser system for simultaneous plaque ablation and fluorescence excitation," *Lasers Surg. Med.* **14**(3), 238–248 (1994).
37. J. J. Baraga, R. P. Rava, P. Taroni, C. Kittrell, M. Fitzmaurice, and M. S. Feld, "Laser-induced fluorescence spectroscopy of normal and atherosclerotic human aorta using 306–310 nm excitation," *Lasers Surg. Med.* **10**(3), 245–261 (1990).
38. A. L. Bartorelli, M. B. Leon, Y. Almagor, L. G. Prevosti, J. A. Swain, C. L. Mcintosh, R. F. Neville, M. D. House, and R. F. Bonner, "*In vivo* human atherosclerotic plaque recognition by laser-excited fluorescence spectroscopy," *J. Am. Coll. Cardiol.* **17**(6), B160–B168 (1991).
39. A. Christov, E. Dai, M. Drangova, L. Y. Liu, G. S. Abela, P. Nash, G. McFadden, and A. Lucas, "Optical detection of triggered atherosclerotic plaque disruption by fluorescence emission analysis," *Photochem. Photobiol.* **72**(2), 242–252 (2000).
40. K. Arakawa, K. Isoda, T. Ito, K. Nakajima, T. Shibuya, and F. Ohsuzu, "Fluorescence analysis of biochemical constituents identifies atherosclerotic plaque with a thin fibrous cap," *Arterioscler., Thromb., Vasc. Biol.* **22**(6), 1002–1007 (2002).
41. G. O. Angheloiu, J. T. Arendt, M. G. Muller, A. S. Haka, I. Georgakoudi, J. T. Motz, O. R. Scepanovic, B. D. Kuban, J. Myles, F. Miller, E. A. Podrez, M. Fitzmaurice, J. R. Kramer, and M. S. Feld, "Intrinsic fluorescence and diffuse reflectance spectroscopy identify superficial foam cells in coronary plaques prone to erosion," *Arterioscler., Thromb., Vasc. Biol.* **26**(7), 1594–1600 (2006).
42. L. Marcu, M. C. Fishbein, J. M. I. Maarek, and W. S. Grundfest, "Discrimination of human coronary artery atherosclerotic lipid-rich lesions by time-resolved laser-induced fluorescence spectroscopy," *Arterioscler., Thromb., Vasc. Biol.* **21**(7), 1244–1250 (2001).
43. L. Marcu, Q. Y. Fang, J. A. Jo, T. Papaioannou, A. Dorafshar, T. Reil, J. H. Qiao, J. D. Baker, J. A. Freischlag, and M. C. Fishbein, "*In vivo* detection of macrophages in a rabbit atherosclerotic model by time-resolved laser-induced fluorescence spectroscopy," *Arteriosclerosis (Dallas)* **181**(2), 295–303 (2005).
44. L. Marcu, J. A. Jo, Q. Fang, T. Papaioannou, T. Reil, J. H. Qiao, J. D. Baker, J. A. Freischlag, and M. C. Fishbein, "Detection of rupture-prone atherosclerotic plaques by time-resolved laser-induced fluorescence spectroscopy," *Arteriosclerosis (Dallas)* **204**(1), 156–164 (2009).
45. S. Tsimikas, "Noninvasive imaging of oxidized low-density lipoprotein in atherosclerotic plaques with tagged oxidation-specific antibodies," *Am. J. Cardiol.* **90**(10), L22–L27 (2002).
46. W. H. Yong, P. V. Butte, B. K. Pikul, J. A. Jo, Q. Y. Fang, T. Papaioannou, K. L. Black, and L. Marcu, "Distinction of brain tissue, low grade and high grade glioma with time-resolved fluorescence spectroscopy," *Front. Biosci.* **11**, 1255–1263 (2006).
47. P. V. Butte, B. K. Pikul, A. Hever, W. H. Yong, K. L. Black, and L. Marcu, "Diagnosis of meningioma by time-resolved fluorescence spectroscopy," *J. Biomed. Opt.* **10**(6), 064026 (2005).
48. Q. Y. Fang, T. Papaioannou, J. A. Jo, R. Vaitha, K. Shastry, and L. Marcu, "Time-domain laser-induced fluorescence spectroscopy apparatus for clinical diagnostics," *Rev. Sci. Instrum.* **75**(1), 151–162 (2004).
49. Y. Sun, R. Liu, D. S. Elson, C. W. Hollars, J. A. Jo, J. Park, Y. Sun, and L. Marcu, "Simultaneous time- and wavelength-resolved fluorescence spectroscopy for near real-time tissue diagnosis," *Opt. Lett.* **33**(6), 630–632 (2008).
50. D. S. Elson, J. A. Jo, and L. Marcu, "Miniaturized side-viewing imaging probe for fluorescence lifetime imaging (FLIM): validation with fluorescence dyes, tissue structural proteins, and tissue specimens," *New J. Phys.* **9**, 127 (2007).
51. W. R. Ware, L. J. Doemeny, and T. L. Nemzek, "Deconvolution of fluorescence and phosphorescence Decay Curves—Least-Squares Method," *J. Phys. Chem.* **77**(17), 2038–2048 (1973).
52. D. V. Oconnor, W. R. Ware, and J. C. Andre, "Deconvolution of fluorescence decay curves—critical comparison of techniques," *J. Phys. Chem.* **83**(10), 1333–1343 (1979).
53. J. M. I. Maarek, L. Marcu, W. J. Snyder, and W. S. Grundfest, "Time-resolved fluorescence spectra of arterial fluorescent compounds: reconstruction with the Laguerre expansion technique," *Photochem. Photobiol.* **71**(2), 178–187 (2000).
54. J. A. Jo, Q. Y. Fang, T. Papaioannou, and L. Marcu, "Fast model-free deconvolution of fluorescence decay for analysis of biological systems," *J. Biomed. Opt.* **9**(4), 743–752 (2004).
55. P. Ashjian, A. Elbarbary, P. Zuk, D. A. DeUgarte, P. Benhaim, L. Marcu, and M. H. Hedrick, "Noninvasive *in situ* evaluation of osteogenic differentiation by time-resolved laser-induced fluorescence spectroscopy," *Tissue Eng.* **10**(3–4), 411–420 (2004).
56. J. M. I. Maarek, L. Marcu, M. C. Fishbein, and W. S. Grundfest, "Time-resolved fluorescence of human aortic wall: use for improved identification of atherosclerotic lesions," *Lasers Surg. Med.* **27**(3), 241–254 (2000).
57. J. A. Jo, Q. Fang, T. Papaioannou, J. D. Baker, A. H. Dorafshar, T. Reil, J. H. Qiao, M. C. Fishbein, J. A. Freischlag, and L. Marcu, "Laguerre-based method for analysis of time-resolved fluorescence data: application to *in vivo* characterization and diagnosis of atherosclerotic lesions," *J. Biomed. Opt.* **11**(2), 021004 (2006).
58. D. N. Stephens, J. Park, Y. Sun, T. Papaioannou, and L. Marcu, "Intraluminal fluorescence spectroscopy catheter with ultrasound guidance," *J. Biomed. Opt.* **14**(3), 030505 (2009).
59. S. Waxman, F. Ishibashi, and J. E. Muller, "Detection and treatment of vulnerable plaques and vulnerable patients: novel approaches to prevention of coronary events," *Circulation* **114**(22), 2390–2411 (2006).
60. L. Marcu, W. S. Grundfest, and M. C. Fishbein, "Time-resolved laser-induced fluorescence spectroscopy for staging atherosclerotic lesions," in *Fluorescence in Biomedicine*, M. A. Mycek and B. Pogue, Eds., pp. 397–430, Marcel Dekker, New York (2003).
61. R. O. Duda, P. E. Hart, and D. G. Stork, *Pattern Classification*, John Wiley and Sons, New York (2004).
62. J. Phipps, Y. Sun, R. Saroufeem, N. Hatami, and L. Marcu, "Fluorescence lifetime imaging microscopy for the characterization of atherosclerotic plaques," *Proc. SPIE* **7161**, 71612G (2009).
63. R. Virmani, A. P. Burke, A. Farb, and F. D. Kolodgie, "Pathology of the vulnerable plaque," *J. Am. Coll. Cardiol.* **47**(8), C13–C18 (2006).